NUCL SCI TECH (2020) 31:3
https://doi.org/10.1007/s41365-019-0717-9

Attenuation coefficients of gamma and X-rays passing through six materials

Xue-Dou Su[1] · Gao-Long Zhang[1,2] · Shou-Ping Xu[3] · Wei-Wei Qu[4] · Lin Song[1] · Yu-Hua Huang[1] · Ben Wang[1] · Yi-Feng Wang[1] · Ze-Tao Zhang[1] · Wu-Fu Xu[1] · Ming-Li Wang[1]

Received: 19 August 2019 / Revised: 16 October 2019 / Accepted: 9 November 2019 / Published online: 19 December 2019

Abstract The aim of this study was to determine the attenuation of gamma and X-rays with different energies caused by passage through different materials. To this end, different materials with a range of atomic numbers were chosen to measure gamma and X-ray attenuation coefficients and to explore the mechanisms of interaction of gamma and X-rays with matter of various kinds. It is shown that the attenuation coefficients first decrease and then increase with increase in the radiation (photon) energy. The attenuation of gamma and X-rays passing through materials with high atomic number is greater than that in materials with low atomic number. The attenuation minimum is related to the atomic number of the irradiated materials. The larger the atomic number is, the lower the energy corresponding to attenuation minimum is. Photoelectric and Compton effects are the main processes when gamma rays pass through individual materials with high and low atomic numbers, respectively. Therefore, for radiotherapy and radiation protection, different methods should be considered and selected for the use of gamma and X-rays of different energies for use in different materials.

Keywords Attenuation coefficient · Interaction mechanisms · Gamma rays · High-energy X-rays · Therapy and protection

1 Introduction

The measurement of gamma and X-ray attenuation coefficients is very important in applied science. This knowledge is invaluable in many fields, such as industry and agriculture [1], and it is especially important in radiotherapy [2–5] and for radiation protection [6–10]. For radiotherapy, generally gamma rays and X-rays are used. X-rays are produced using the bremsstrahlung method, which involves electron beams hitting a target material with high atomic number. Owing to their strong pass-through characteristic, gamma and X-rays have been developed for use in Gamma Knife and X-ray radiation machines for the treatment of tumor cells with non-invasive therapy [11, 12]. However, during the therapy procedure, when these rays pass through normal tissues, they also kill normal cells in the irradiated region [13, 14]. Moreover, gamma and X-rays with different energies are used for different tissues. It is very important to know how to use these rays effectively and safely [15, 16].

When photons interact with the atoms in matter, the major processes that occur are the photoelectric effect, Compton effect, and pair production [17, 18]. The photons that interact with the atoms in matter are absorbed or

This work was supported by the National Natural Science Foundation of China (Nos. 11475013, 11975040 and U1832130).

✉ Gao-Long Zhang
zgl@buaa.edu.cn

[1] School of Physics and Nuclear Energy Engineering, Beihang University, Beijing 100191, China

[2] Beijing Advanced Innovation Center for Big Data-Based Precision Medicine, Beihang University, Beijing 100083, China

[3] Department of Radiation Oncology, PLA General Hospital, Beijing 100853, China

[4] State Key Laboratory of Radiation Medicine and Protection, School of Radiation Medicine and Protection, Soochow University, Suzhou 215123, China

scattered and have their energies changed and trajectories deflected from their original directions. Probabilities are denoted by cross section to describe these three effects. When gamma and X-rays pass through matter, their intensity weakens, and this process is represented by [19]

$$I = I_0 e^{-\sigma_\gamma N x}. \quad (1)$$

Here, I_0 and I are the intensity of gamma and X-rays before and after passing through matter, respectively. N and x are the atomic numbers per unit area and thickness of the matter, respectively. $\sigma_\gamma N = \mu$ is the linear attenuation coefficient. σ_γ is the sum of the cross sections of the photoelectric effect, Compton effect, and pair production. Then, $I = I_0 e^{-\mu x}$, where the unit of x is cm and the unit of μ is cm^{-1}. This is because $N = (\rho/A)N_A$, μ is related to the matter density ρ. The term A is the atomic mass number of a material and N_A is Avogadro's number.

For μ research, several studies were performed [20–22] to investigate the correlation of μ with beam width, matter shape, etc. Some μ were measured to study the properties of new materials, such as the effect of antimony oxide [23], the application of low- and high-energy photons [24], and shielding against gamma and X-rays [25]. Similarly, it was found that some new materials have the potential to reduce gamma and X-rays better than lead does and could be used as shielding materials. Transparent and non-toxic forms of glass may replace the common radiation shielding concrete and lead-based commercial glass used for gamma ray shielding applications [26]. Some Al-based glassy alloys were found to be good materials for shielding from gamma radiation [27]. Some newly developed materials were explored to verify their potential as gamma ray shielding by calculating their radiation attenuation coefficients [28, 29]. The mass attenuation coefficients of soil and sediment samples were measured in studies of soil properties for agricultural uses of gamma rays with energies from 46.5 to 1332 keV [30, 31]. Moreover, some fruits were studied under different storage times and physiological conditions to explore the absorption of different food components [32]. The studies above were mainly focused on investigation of the radiation properties of new materials and their use for gamma ray shielding. The application of μ to medical physics still needs to be explored. It is well known that the cross sections of the photoelectric, Compton, and pairs effects change with the gamma/X-ray energy and the atomic number of the matter; hence, μ also changes with them. However, how the change occurs needs to be explored. In this paper, we introduce the results of a study on the attenuation of gamma and X-rays with different energies in different materials, especially two kinds of materials particularly applicable for radiotherapy.

This paper is organized as follows. Section 2 describes the experimental procedure. The data analysis and discussions are presented in Sect. 3. The summary is given in Sect. 4

2 Experiment

A schematic diagram of the experimental setup is shown in Fig. 1. It was composed of radioactive sources, NaI (Tl) scintillation detector, high-voltage power module, spectroscopy amplifier, multi-channel analyzer (MCA), and computer and absorption equipment. The radioactive sources included ^{137}Cs, ^{60}Co, ^{22}Na, ^{133}Ba, and ^{152}Eu, which produce gamma rays in the energy range 54–1408 keV. The absorption pieces included Pb, Cu, Fe, Al, RW3 solid water (PTW, Germany), and poly-methyl methacrylate (PMMA) materials. The last two materials are equivalents of human tissue and are used to simulate human tissues in radiotherapy. The detector, sources, and materials were placed in a lead box to decrease the background. A collimator and a slit, respectively, were placed in front of the radioactive sources so that the detector can obtain a parallel beam and decrease the scattering counts. The gamma rays produced by radioactive sources passed through these pieces and interacted with matter. When high voltage power provides high voltage to a NaI(Tl) detector, the detector outputs the signals. The energies of the gamma rays passing through matter were converted into photons in the crystal and then converted to electrical signals in a photomultiplier tube in the detector. Then, the signals were amplified by a spectroscopy amplifier, imported into the MCA module, and transformed by A/D conversion. This module was connected to a computer; hence, the final results are indicated on a computer interface, e.g., energy spectra are obtained.

High-energy X-rays were produced by Varian Clincal IX5230 and Elekta Synergy linear accelerator of People's Liberation Army (PLA) General Hospital in Beijing. In the medical electron linear accelerator, electrons were produced by an electron gun and then accelerated by allowing them to interact with microwaves in a microwave-

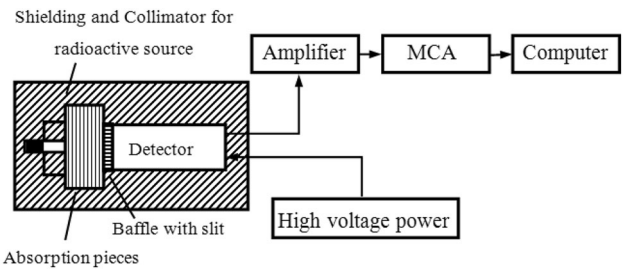

Fig. 1 Schematic of the experimental setup

accelerated waveguide tube. Then, in a deflection magnetic field, these electrons were aligned to form an electron beam and emitted from an electron window to hit a tungsten metal target. This produced a large number of high-energy X-rays. In this experiment, electron beams with 6 MeV, 10 MeV, 15 MeV, and 18 MeV were selected.

The high-energy X-rays passed though the absorption pieces and interacted with matter. The X-rays passing though the pieces irradiated EBT3, which is a special film that responds based on the radiation cross-linking effect. This causes discoloration (clouding) of the plastics and reflects the dose received. When different doses of X-rays irradiated the EBT3, the film darkness was different: The larger the X-ray dose, the darker the film was. After X-ray irradiation, the film was scanned using a commercial flat-bed scanner. This caused the degree of irradiation recorded in the film to be transformed into a grayscale image. Therefore, the larger the dose of X-ray irradiation of the film was, and the larger the grayscale of the scanned image was. The dose-grayscale calibration curve of the film was obtained by measuring the grayscale of the film corresponding to the known dose of X-rays and making a polynomial fit, as shown in Fig. 2. Thus, it was possible to determine the dose of the X-rays that passed though the matter using the grayscale image from the film. Moreover, when the X-rays passed through the matter, the X-ray dose was weakened, which is represented by

$$D = D_0 e^{-\mu x}. \quad (2)$$

Here, D_0 and D are the doses of X-rays before and after they passed through the matter, respectively. The term x is the thickness of the absorption pieces.

3 Results and discussion

The energy spectra of gamma rays from a ^{60}Co radioactive source on Pb and RW3 solid water pieces are shown in Fig. 3. Excluding a wide peak for background at lower energies, it is observed from Fig. 3a that the peaks can be clearly observed at higher energies. However, in Fig. 3b, the counts have a smoothly continuous distribution; thus, no peaks were observed at higher energies. Gamma rays passing through materials with high atomic number readily cause the photoelectric effect and for materials with low atomic number, gamma rays readily cause the Compton effect [33]. The lead and RW3 solid water pieces are materials with high and low atomic numbers, respectively. Therefore, for the lead piece, photoelectric peaks can be observed, and for RW3 solid water piece, the Compton effect produced scattered gamma rays with continuous energies. Finally, when gamma rays interact with different materials, the three kinds of effects make different contributions.

Under the same experimental conditions, the gamma ray intensity is proportional to the gamma ray count N, hence $N = N_0 e^{-\mu x}$, thus

$$\ln N = \ln N_0 - \mu x. \quad (3)$$

The absolute value of the slope of this line is μ. For experimental data, we only plot the function $\ln N$ with the variable x, then fit it to a linear function to obtain μ. A sample of this process is shown in Fig. 4 for the Pb and Al pieces. Here, the statistical error is considered, which was about 0.6–1.5%. Using the same method for high-energy X-rays by measuring the absorption dose after entering different materials with different thickness, the μ values were obtained.

According to the above method, we obtained the μ values of six types of materials with different gamma ray energies, which are shown in Fig. 5. As seen from Fig. 5, the attenuation coefficients decreased with increase in the

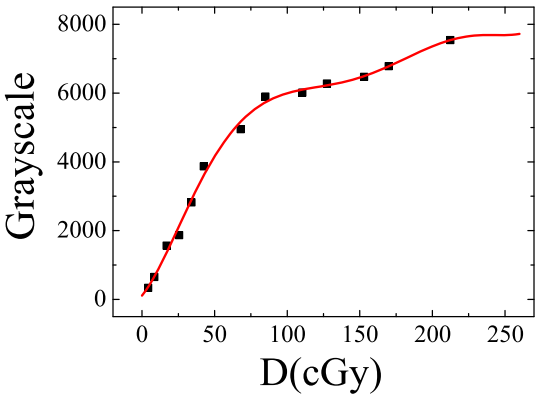

Fig. 2 Experimental data and curve of the grayscale with absorption dose. The grayscale has no unit

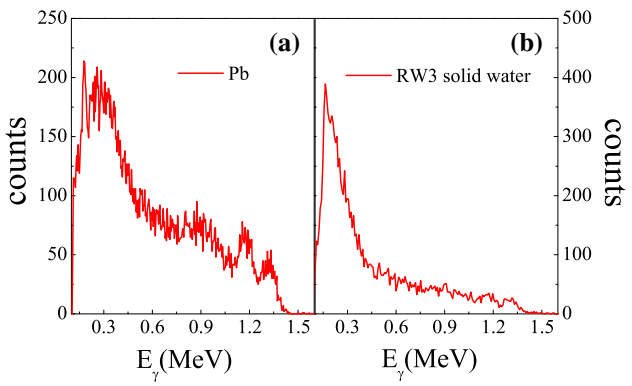

Fig. 3 Energy spectra of gamma rays from ^{60}Co radioactive sources that passed through **a** Pb and **b** RW3 solid water pieces

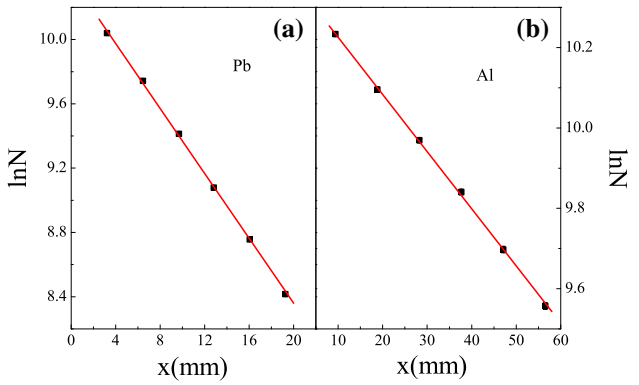

Fig. 4 Plots of the attenuation curves of the Pb and Al pieces. The fitting results are indicated by the solid line

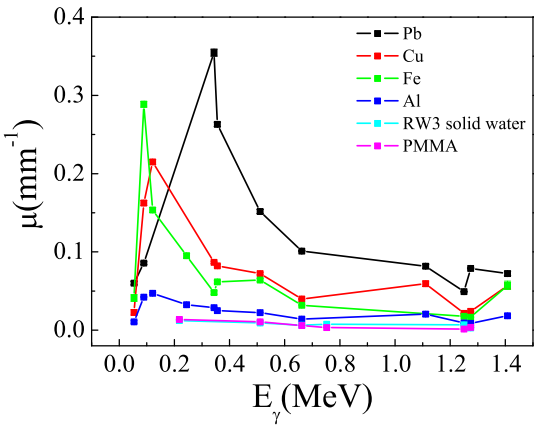

Fig. 5 μ values of different materials in relation to gamma ray energy

gamma ray energy from 100 keV to several MeV. However, when the gamma ray energy was less than 100 keV, the μ of the Pb material significantly decreased at 80 keV owing to the resonance absorption of gamma rays. The μ of Cu, Fe, and Al materials also showed significant decrease at 50 keV. Moreover, the μ of Pb, Cu, Fe, Al, RW3 solid water, and PMMA materials decreased sequentially with decrease in the atomic number of those materials. It is shown that the μ value depends on the gamma ray energy. In the present range of the gamma energy, the μ value decreases with increase in the gamma ray energy. Moreover, μ is related to the density and atomic number of matter. The attenuation of gamma rays in materials with high atomic number is greater than that in materials with low atomic number.

The μ values of six types of materials with high-energy X-rays are indicated in Fig. 6a, together with the data from Fig. 5. We can see that in connection with the trend of μ values of different materials for gamma rays, the different trends of six types of materials are observed for high-energy X-rays. On the whole, with increase in the photon energy, the μ values show a decreasing trend. Thus, the

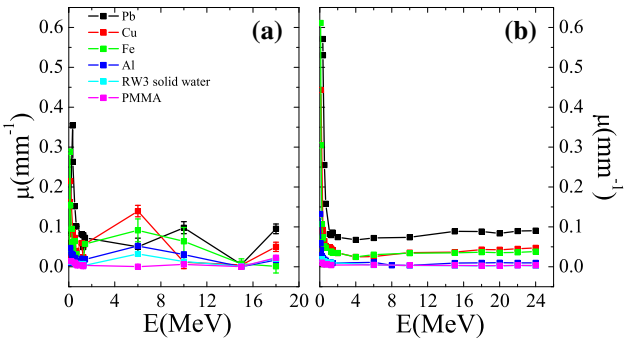

Fig. 6 μ values of different materials with gamma ray and high-energy X-ray energy. **a** Experimental data and **b** simulation results

attenuation coefficient depends on the photon energy. When the energy is more than 15 MeV, all the μ values increase; moreover, those of Pb and Cu increase more quickly. When the energies are less than 15 MeV and more than 2 MeV for Pb, the μ values first decrease, then increase and decrease again. For Cu, Fe, and Al, the μ values first increase and then decrease. However, the values of Cu increase and decrease most quickly. The ones for Al increase and decrease most slowly. The μ values of Fe lie between those of Cu and Al. For RW3 solid water and PMMA, the μ values do not change much and remain nearly constant. According to the comparison, the μ values first decrease with increase in photon energies and tend to one minimum, then increase with increase in the photon energy. The μ values of Pb decrease most quickly and those of RW3 solid water and PMMA decrease most slowly. For Pb, the μ minimum tends toward lower energy; however, for Al, RW3 solid water, and PMMA, the μ minimum tends to higher energy. Thus, at μ, the minimum corresponding photon energy is related to the atomic number of the material. The corresponding photon energy tends to be lower with increase in the atomic number of the material. Owing to the existence of the μ minimum, there are gamma and X-ray components that are not easily attenuated; these are called the hard components of gamma and X-rays. These parts appear near the μ minimum. In regards to shielding and protection, these hard components are not beneficial.

To further verify the above conclusion, a Monte Carlo simulation (GEANT4 toolkit [34] with version 10.5) was performed to calculate the attenuation coefficient of the six types of materials discussed previously. To obtain the attenuation coefficients, we simulated the process in which gamma rays and high-energy X-rays with different energies passed through the six types of material. The absorption pieces were cuboids of fixed length and width, but with different thickness (similar to the absorption pieces used in the experiment). The point radioactive source and a fixed number of photons were used in the simulation. In a three-

dimensional coordinate space, the radioactive source was set as the center of mass of the absorption pieces. The thickness, length, and width of the absorption piece were along the X, Y, and Z directions, respectively. The radioactive source was located at a point on the X-axis. The position of the point was fixed and sufficiently far from the radioactive source. Therefore, the radioactive source was always outside the absorption pieces when the thickness of the absorption pieces increased. Then, we input one type of material and the photon energy that we had measured, and then, we changed the thickness of the absorption pieces. The number of photons passing through the absorption pieces was counted. After we determined the number of photons, we calculated the attenuation coefficient using the method shown in Fig. 4.

The calculation results are shown in Fig. 6b. We can see that the trends of the calculations are consistent with those of the experimental data for the μ values of gamma rays and high-energy X-rays on different materials. First, the μ values of different materials decrease with increase in the energy. After the μ values tend to a minimum, they then begin to increase with increase in energy until they reach 20 MeV. The larger the atomic number is, the lower the energy corresponding to attenuation coefficient minimum is. When the photon energy is more than 20 MeV, the μ values of Pb, Cu, Fe, Al, RW3 solid water, and PMMA materials decrease sequentially with decrease in atomic number. However, the μ value did not change significantly for every material. It is shown that the attenuation coefficients depend on the energy of rays and atomic number of materials, which is consistent with the experimental conclusions. Thus, the simulation results supported the experimental conclusions.

4 Summary

On the basis of the above results, it was shown that the attenuation coefficients of gamma rays and high-energy X-rays for different materials depend on the photon energy and atomic numbers of the materials. The larger the atomic number of a material, the more quickly the attenuation of gamma and X-ray intensity decreased. The attenuation of gamma and X-rays in materials with high atomic number was greater than that in materials with low atomic number. When the photon energy was more than 2 MeV and less than 15 MeV, the attenuation first increased and then decreased with increase in the photon energy. Thus, an attenuation minimum exists. The corresponding photon energy was related to the atomic number of the material. The larger the atomic number was, the lower the energy corresponding to attenuation minimum was. For protection from gamma and X-rays, materials including nuclear elements with high atomic number should generally be selected. The hard components in the gamma and X-rays should be diminished. For gamma rays in the energy ranges of several hundred keV to 1 MeV, the photoelectric and Compton effects are the main processes of gamma rays in individual materials with high and low atomic numbers. The gamma and X-ray energy produced different effects. In the fields of gamma and X-ray therapy and protection, different methods should be considered and selected for gamma and X-rays with different energies in different materials.

References

1. S.Z. Luo, *Application of Nuclear Technology* (Harbin Engineering University Press, Harbin, 2009). **(in Chinese)**
2. M.D. Bethesda, Structural shielding design for medical imaging X-ray facilities. Phys. Med. Biol. **50**, 4243–4244 (2005). https://doi.org/10.1088//0031-9155/50/17/B01
3. K.P. Adhikari, A medical physics perspective: radiation therapy in Nepal. Med. Phys. Int. J. **6**, 145–147 (2018)
4. E. Rosenblatt, Planning national radiotherapy services. Front. Oncol. (2014). https://doi.org/10.3389/fonc.2014.00315
5. A.W. Lightstone, S.H. Benedict, F.J. Bova et al., Intracranial stereotactic positioning systems: report of the American Association of Physicists in Medicine Radiation Therapy Committee Task Group No. 68. Med. Phys. **32**, 2380–2398 (2005). https://doi.org/10.1118/1.1945347
6. A.A. El-Sayed, M.A. El-Sarraf, F.A. Gaber, Utilization of ilmenite/epoxy composite for neutrons and gamma rays attenuation. Ann. Nucl. Energy **30**, 175–187 (2003). https://doi.org/10.1016/s0306-4549(02)00052-X
7. R. Allen, S.C. Edwards, The repair of concrete structures. Cem. Concrete Assoc. **22**, 125–138 (1987). https://doi.org/10.1080/00218468708074996
8. H.S. Hu, Q.S. Wang, J. Qin et al., Study on composite material for shielding mixed neutron and γ-rays. IEEE Trans. Nucl. Sci. **55**, 2376–2384 (2008). https://doi.org/10.1109/TNS.2008.2000800
9. S. Kaur, K.J. Singh, Investigation of lead borate glasses doped with aluminum oxide as gamma ray shielding materials. Ann. Nucl. Energy **63**, 350–354 (2014). https://doi.org/10.1016/j.anucene.2013.08.012
10. M. Kozlovska, R. Cerny, P. Otahal, Attenuation of X and gamma rays in personal radiation shielding protective clothing. Radiat. Saf. J. **109**, S205–S211 (2015). https://doi.org/10.1097/HP.0000000000000361
11. K. Vance, A. Ozer, A. Salahuddin, H. Sabbi, Dosimetric comparison of intracranial metastasis treatment using two radiosurgery systems: TrueBeam STx with VMAT and Gamma Knife Model 4C. J. Radiosurg. SBRT **4**, 235–243 (2016)
12. L.S. Chin, S. DiBiase, Radiation necrosis following gamma knife surgery: a case-controlled comparison of treatment parameters and long-term clinical follow up. J. Neurosurg. **94**, 899–904 (2001). https://doi.org/10.3171/jns.2001.94.6.0899
13. G. Kragl, S. AfWetterstedt, B. Knäusl et al., Dosimetric characteristics of 6 and 10 MV un-attened photon beams. Radiother. Oncol. **93**, 141–146 (2009). https://doi.org/10.1016/j.radonc.2009.06.008

14. U. Titt, O.N. Vassiliev, F. Pönisch, L. Dong, H. Liu, R. Mohan, A flattening filter free photon treatment concept evaluation with Monte Carlo. Med. Phys. **33**, 1595–1602 (2006). https://doi.org/10.1118/1.2198327
15. Q.S. Zheng, G.Y. Yu, X. He, M. Jiang, X.F. Chu, S.Y. Zhao, S.J. Fan, P.X. Liu, Protective effect of S-isopentenyl-L-cysteine against DNA damage in irradiated mice. Acta Acad. Med. Sin. **37**, 496–500 (2018). https://doi.org/10.3881/j.issn.1000-503X.2015.05.002
16. M.I. Koukourakis, D. Pitsiava, A. Giatromanolaki et al., Amifostine-related fever-rash during fractionated radiotherapy: diagnostic and predictive role of C-reactive protein. Am. J. Clin. Oncol. **34**, 281–285 (2011). https://doi.org/10.1097/COC.0b013e3181dea7bd
17. X.H. Li, *Radiation Radiology and Protection* (Atomic Energy Press, Beijing, 1980), pp. 17–23
18. R.D. Evans, Energy dependence of the various gamma-ray interaction processes in sodium iodide, in *The Atomic Nucleus*, ed. by R.D. Evans (the McGraw-Hill Book Company, New York, 1955)
19. X.T. Lu, D.X. Jiang, Y.L. Ye, *Nuclear Physics*, vol. 63 (Atomic Energy Press, Beijing, 2000)
20. J.I. Byun, J.Y. Yun, A calibration transmission method to determine the gamma-ray linear attenuation coefficient without a collimator. Appl. Radiat. Isot. **102**, 70–73 (2015). https://doi.org/10.1016/j.apradiso.2015.05.006
21. B.S. Sidhu, A.S. Dhaliwal, K.S. Mann, K.S. Kahlon, Simplified two media method: a modified approach for measuring linear attenuation coefficient of odd shaped archaeological samples of unknown thickness. Appl. Radiat. Isot. **69**, 1516–1520 (2011). https://doi.org/10.1016/j.apradiso.2011.06.007
22. J. Van Dyk, Broad beam attenuation of cobalt-60 gamma rays and 6-, 18-, and 25-MV X-rays by lead. Med. Phys. **13**, 105–110 (1986). https://doi.org/10.1118/1.595929
23. A.M. Zoulfakar, A.M. Abdel-Ghany, T.Z. Abou-Elnasr, A.G. Mostafa, S.M. Salem, H.H. El-Bahnaswy, Effect of antimony-oxide on the shielding properties of some sodium–boro silicate glasses. Appl. Radiat. Isot. **127**, 269–274 (2017). https://doi.org/10.1016/j.apradiso.2017.05.007
24. M.F.M. Yusof, P.N.K. Abd Hamid, Abd.A. Tajuddin, R.H.S. Bauk, N.M. Isa, M.J.Md. Isa. Mass attenuation coefficient of tannin-added *Rhizophora* spp. particleboards at 16.59–25.56 keV photons, and 137Cs and 60Co gamma energies. Radiol. Phys. Technol. **10**, 331–339 (2017). https://doi.org/10.1007/s12194-017-0408-3
25. B. Mavi, F. Gurbuz, H. Ciftci, I. Akkurt, Shielding property of natural biomass against gamma rays. Int. J. Phytorem. **16**, 247–256 (2014). https://doi.org/10.1080/15226514.2013.773276
26. P. Kaur, K.J. Singh, S. Thakur, P. Singh, B.S. Bajwa, Investigation of bismuth borate glass system modified with barium for structural and gamma-ray shielding properties. Spectrochim. Acta Part A Mol. Biomol. Spectrosc. **206**, 367–377 (2018). https://doi.org/10.1016/j.saa.2018.08.038
27. H.C. Manjunatha, L. Seenappa, B.M. Chandrika, K.N. Sridhar, Gamma, X-ray and neutron shielding parameters for the Al-based glassy alloys. Appl. Radiat. Isot. **139**, 187–194 (2018). https://doi.org/10.1016/j.apradiso.2018.05.014
28. K.S. Mann, J. Singla, V. Kumar, G.S. Sidhu, Verification of some building materials as gamma-ray shielding. Radiat. Prot. Dosim. **151**, 183–195 (2012). https://doi.org/10.1093/rpd/ncr455
29. N. Damla, H. Baltas, A. Celik, E. Kiris, U. Cevik, Calculation of radiation attenuation coefficient, effective atomic numbers and electron densities for some building materials. Radiat. Prot. Dosim. **150**, 541–549 (2012). https://doi.org/10.1093/rpd/ncr432
30. M.S. Al-Masri, M. Hasan, A. Al-Hamwi, Y. Amin, A.W. Doubal, Mass attenuation coefficients of soil and sediment samples using gamma energies from 46.5 to 1332 keV. J. Environ. Radioactiv. **116**, 28–33 (2013). https://doi.org/10.1016/j.jenvrad.2012.09.008
31. D. Demir, A. Ün, M. Özgül, Y. Sahin, Determination of photon attenuation coefficient, porosity and field capacity of soil by gamma-ray transmission for 60, 356 and 662 keV gamma rays. Appl. Radiat. Isot. **66**, 1834–1837 (2008). https://doi.org/10.1016/j.apradiso.2008.04.023
32. S. Ghosh, M.K. Das, Attenuation coefficients and absorbed gamma radiation energy of different varieties of potato, mango and prawn at different storage time and physiological condition. Food Chem. **145**, 694–700 (2014). https://doi.org/10.1016/j.foodchem.2013.08.080
33. F. Glenn, *Knoll, Radiation Detection and Measurement*, 3rd edn. (Wiley, New York, 2000), pp. 308–312
34. S. Agostinelli, J. Allison, K. Amako et al., Geant4-simulation toolkit. Nucl. Instrum. Methods Phys. Res. A **506**, 250–303 (2003). https://doi.org/10.1016/S0168-9002(03)01368-8